RSC Advances

ROYAL SOCIETY OF CHEMISTRY

www.rsc.org/advances

Exploring Thermodynamically Downhill Nanostructured Peptide Libraries: From Structural to Morphological Insight

*Dnyaneshwar B. Rasale, Sagar Biswas, Maruthi Konda and Apurba K. Das**

Department of Chemistry, Indian Institute of Technology Indore, Indore, 452017, India.

* To whom the correspondence should be addressed:

Dr. Apurba K. Das, Email: apurba.das@iiti.ac.in

Abstract

Here, we report biocatalytic evolution of Nmoc (naphthalene-2-methoxycarbonyl)-capped dynamic combinatorial peptide libraries in the hydrogel state. Our approach is to use a biocatalyst, which can bring up the peptide self-assembly via synthesis and *in situ* self-organization of peptide oligomers in physiological conditions. The enzyme pools amplification of Nmoc-capped peptide oligomers and leads to generate dynamic combinatorial libraries under physiological conditions via reverse hydrolysis reaction. The enzyme permits reversible peptide synthesis as well as peptide hydrolysis reactions, which lead to generate a preferred nanostructured component through peptide self-assembly. Nmoc-F/FF and Nmoc-L/LL systems have been used successfully to generate Nmoc-F_3 and Nmoc-L_5 as preferred components in the dynamic peptide libraries, which form helical nanostructures. The control experiment with Nmoc-L/LLL system depicts the selection and preferred formation of Nmoc-L_5 library member via self-assembly. The library components are analysed by reverse phase high performance liquid chromatography (RP-HPLC) and mass spectrometry. The self-assembled nanomaterials are studied by rheology, fluorescence and time correlated single photon counting (TCSPC) spectroscopy. The secondary structure of peptide components are analysed by FT-IR and circular dichroism (CD) spectroscopy. The self-assembled nanostructures are imaged by atomic force microscopy (AFM) and transmission electron microscopy (TEM).

Keywords: self-assembly, peptide, nanostructure, preferred component, DCL

Introduction

Self-assembled amphiphilic peptides[1-3] have been used in constructing nanostructured biomaterials due to their potential applications in drug delivery[4-7] and biomedical applications.[8-9] Self-assembly is the result of non-covalent interactions including π-π stacking, hydrogen bonding and hydrophobic interactions of self-assembled molecules. Low molecular weight amphiphilic small molecules can entrap > 99% of water and form supramolecular hydrogel.[10-13] Hydrogel is composed of complex three dimensional nanofibrillar networks,[14-15] which can entrap large volumes of water. Small peptide amphiphiles are used to design self-supporting hydrogels with more ordered nanostructures.[16] Enzyme catalyzed hydrogelation is more promising due to their broad biomedical and nanotechnological applications.[17-19]

Over the last few years, dynamic combinatorial libraries (DCLs)[20-22] of small molecules have emerged as powerful tools to evolve complex nanostructures. The library components undergo continuous bond breaking and making under thermodynamic control, which allows the system to reach an equilibrium state. In a DCL, the inter-conversion of library members occurs through a reversible chemical reaction, which can introduce new covalent[23-25] and non-covalent interactions. Self-assembly driven dynamic libraries are generated under various external stimuli including metal ions,[26] chemical templates,[27] temperature[28] and enzymes.[29] External stimuli can drive the library members to reorganize in a particular fashion in order to minimize the total free energy of the system. Typically, enzymes are used to hydrolyse the polymers for controlled drug delivery applications.[30] Enzymes mainly proteases are also used to exploit the peptide self-assembly via reverse hydrolysis reactions.[31-33] The self-assembling peptide hydrogel systems are also achieved via lipase catalysed reverse hydrolysis reactions.[34-35] Steroidal motifs were used to generate hydrazone based DCLs.[36] Otto *et al* described peptide based dynamic combinatorial

libraries based on disulfide exchange reaction.[37] Lehn *et al* envisaged constitutional dynamic hydrogel based on self-assembly and reversible connection of library components.[38] The stabilization of a library component among the library members depends on the formation of stable assemblies or aggregates. In the pool of enzymatic chemical reactions, the self-assembly of a library component shifts the equilibrium towards its formation. This results in the amplification of a preferred self-assembled component over the less or dis-assembled components. Previously, N-terminus of amino acids or peptides were functionalized with aromatic fluorenyl methoxycarbonyl (Fmoc-) group,[39-40] which play crucial role in the self-assembly process. Ulijn *et al.* reported fully reversible self-assembly of small low molecular weight peptides under thermodynamic control.[32] Palocci *et al*. described the use of microbial lipases for the synthesis of Fmoc-tripeptide results in the formation of gel.[34] Recently, we have explored π-stacked *β*-sheet dynamic peptide libraries through the hydrolysis of peptides, which is catalysed by an enzyme.[41]

In here, our attention is to explore enzyme catalysed dynamic peptide libraries where a protease enzyme can bring up the self-assembly of peptides through reverse hydrolysis of aromatic Nmoc (naphthalene-2-methoxycarbonyl)-capped amino acids and dipeptides. Naphthalene-based peptides are an interesting class of low molecular weight gelators, which have been used in cell culture,[42] energy transfer[43] and drug delivery[5] applications. Here, we report enzymatic reactions of Nmoc-amino acids with a variety of dipeptides or a tripeptide, which lead to generate dynamic combinatorial libraries and consequently self-assembly can drive the amplification of a library component among the library members. The thermodynamic stabilization of a preferred library component in gel phase medium forms complex nanostructure.

Results and Discussion

Nmoc-amino acids (Phe: F, Leu: L, Val: V and Ala: A), dipeptides (FF, LL, VV and AA) and tripeptide (LLL) were synthesized to generate dynamic combinatorial libraries in aqueous medium (Scheme 1, S1, S2 and S3). Dynamic combinatorial chemistry is a powerful tool to generate complex nanostructure in supramolecular hydrogel. We have carried out enzyme catalysed reverse hydrolysis reaction with Nmoc-protected amino acids and dipeptides to generate dynamic combinatorial libraries. Nmoc-F/FF (20:60 mmol L^{-1}) and Nmoc-L/LL (20:60 mmol L^{-1}) were dissolved in 2 mL phosphate buffer (100 mmol, pH~ 8) respectively. The milky suspension was mixed to make homogeneous solution and kept undisturbed at room temperature. The self-assembly through enzymatic chemical reaction was observed (Figure 1), when the enzyme thermolysin 1 mg/mL was added to the respective solution (Table 1). The self-assembled self-supporting hydrogelation was observed within 5 min for Nmoc-F/FF system with 40% conversion of Nmoc-F_3. However, Nmoc-L/LL system took around 36 h to form a self-assembled hydrogel. The HPLC analysis exhibits the formation of Nmoc-based peptide oligomers, which clearly indicates the selectivity of enzyme towards reverse hydrolysis reaction. The newly synthesized library components were confirmed by HPLC and ESI-MS (Figures S1-S12). Nmoc-F_3 was formed as a major component in the self-assembled Nmoc-F/FF hydrogel system with 71% conversion, whereas Nmoc-L_5 formed predominantly with 44% conversion for the self-assembled Nmoc-L/LL hydrogel system (Figure 2). In here, Nmoc-F_3 of Nmoc-F/FF system and Nmoc-L_5 of Nmoc-L/LL system are the self-assembled component over the other non-assembled components. Our enzyme catalysed amplification of Nmoc-L/LL and Nmoc-F/FF results are very similar with the results[32] of Fmoc-L/LL and Fmoc-F/FF[34-35] systems.

The enzyme catalysed newly synthesised Nmoc-F_3 and Nmoc-L_5 oligomers self-assembled in aqueous medium and turned to hydrogels. However, to evaluate the amplification of self-assembled components in dynamic libraries, the Nmoc-F/FF and Nmoc-L/LL systems were studied at different concentrations. Nmoc-F/FF system at lower concentration (5:15 mmol L^{-1}) showed random distribution of library components and all the library components remained in solution form while Nmoc-L/LL system didn't show peptide conversion upon enzyme addition at lower (5:15 mmol L^{-1}) concentration (Figure 3). Moreover, increase in concentration from 5 to 20 mmol L^{-1} of Nmoc-amino acids, Nmoc-F_3 and Nmoc-L_5 were formed as a preferred component for Nmoc-F/FF and Nmoc-L/LL systems respectively. Nmoc-L/LL system led to form Nmoc-L_5 by subsequent coupling of dipeptide LL with Nmoc-L, which results in the self-assembly. However, preferred components or library members self-organize or self-assemble at their minimum energy state. This was clearly demonstrated by a control experiment with Nmoc-L/LLL system. In this case, Nmoc-L_4 was generated by Nmoc-L/LLL system with 52% conversion which was collapsed over time and Nmoc-L_5 was dominated in the DCL pool (Figure 4). Thus, self-assembly provides driving force for generation and self-selection of peptides via breaking and making of peptide bonds in protease triggered dynamic combinatorial libraries. The Nmoc-L/LLL system proves that self-assembly drives the formation of thermodynamically stable product among the library members (Figure 5). Nmoc-V/VV and Nmoc-A/AA systems were unable to form hydrogel and no product conversion was observed.

In order to generate a more complex system and evolve unexpected library member Nmoc-L was mixed with LL, VV, AA and GG dipeptides. The library members Nmoc-L_5 (20%), Nmoc-LLVV (19%) and Nmoc-LLLVV (12%) were formed after 10 days (Figure 6). In here, two

different major peptide oligomers Nmoc-L_5 and Nmoc-LLVV were unable to form self-supporting hydrogel, indicating no supramolecular arrangement among different peptide oligomers. This complex Nmoc-L/LL/VV/AA/GG system led to form more complex reaction products and unable to self-assemble due to random distribution of library components. Our results in Nmoc-L/LL system showed that Nmoc-L can couple with LL but unable to couple with other dipeptides VV, AA and GG. However, the synthesized Nmoc-LL and Nmoc-LLL coupled with VV and form Nmoc-LLVV and Nmoc-LLLVV peptides (Figure S13-S15). Thus, our result indicates that protease catalysed amplification drives towards a preferred product formation (Figure 6).

The peptide self-assembly in the DCLs is influenced by various non-covalent interactions. The hydrogen bonding interactions of amide bonds play crucial role in the self-assembly process, which is responsible for peptide secondary structures. Therefore, FTIR is used to monitor the secondary structure of peptides. The self-assembled peptides acquire a particular secondary structure, which can be elucidated based on amide I region (C=O stretching vibration of amide bond) in FTIR. Oxygen atom of C=O of amide bonds acts as donor in hydrogen bonding interactions in the peptide self-assembly. The self-assembled structure from Nmoc-F/FF and Nmoc-L/LL systems showed characteristic peaks in the amide I region. A preferred library component Nmoc-F_3 was responsible for self-supporting hydrogel of Nmoc-F/FF system. The peptide Nmoc-F_3 showed peaks at 1636 cm^{-1} and 1689 cm^{-1} in FTIR, which indicate antiparallel β-sheet structure in the self-assembled hydrogel state[44-46] (Figure 7). Moreover, Nmoc-L_5 was obtained preferentially from Nmoc-L/LL system, which was responsible for hydrogel formation. The preferred library member Nmoc-L_5 exhibited a characteristics peak at 1636 cm^{-1} in the

amide I region (Figure 7). The presence of the peak indicates that two peptide backbones are held together by hydrogen bonding interactions, which is responsible for β-sheet conformation. The self-organization at the molecular level establishes β-sheet structure, which forms helical structure at the higher level molecular self-assembly.

Circular Dichroism (CD) measurement was also done to better assess the nature of the secondary structure of the self-assembled peptides. The CD spectrum of Nmoc-F/FF system shows characteristic negative peaks at 222 nm and 212 nm, which are attributed from n-π* transition of the CONH groups of peptide Nmoc-F_3. This signature is analogous to the reported CD signature of peptides adopting typical helical conformation (Figure 8).[47-49] The helical conformation of peptide nanostructures is consistent with results of atomic force microscopy. The CD analysis for Nmoc-L/LL system interestingly shows β-sheet and helical structures. The characteristic negative peak was observed at 219 nm and a positive peak appeared at 203 nm (Figure 8). This observation indicates that the gelator molecules self-assembled [50-54] into β-sheet and helical structures through extensive hydrogen-bonding interactions.

Fluorescence study of hydrogels **1** and **2** was carried out to get more insight into the molecular arrangement of self-assembled peptides. UV-Vis absorbance spectra were recorded to know the exact excitation wavelength of hydrogels **1** and **2** (Figure S16). Aromatic π-stacking interaction[55-57] is known to be the driving force behind the self-assembly of aromatic peptide amphiphiles. Aromatic Nmoc (naphthalene-2-methoxycarbonyl)-protected peptide hydrogels **1** and **2** exhibit strong emission peak at 346 nm and 341 nm respectively (Figure S17). The emission at 346 nm and 341 nm for hydrogels is attributed from the π-stacking interaction of

aromatic naphthalene rings in hydrogel state. The emission at 465 nm has been observed for hydrogel **1**. The emission at 465 nm indicates excimer formation of Nmoc groups in gel phase. The emission peaks for both hydrogels indicate that multiple naphthalene moieties aggregate through π-stacking interactions.

Time resolved fluorescence spectra were recorded to investigate the higher order aggregated state of the fluorophore groups in the hydrogel system (Figure 9). The fluorescent decay profile has been fitted to the equation given below

$$\langle \tau \rangle = \sum_{i=1}^{n} a_i \tau_i$$

where τ_i is the fluorescence lifetime of various fluorescent species and a_i is the pre-exponential factors. All curves have been fitted with tetra exponential decay curve. The time resolved fluorometry allows very keen discrimination between fluorophore species in different environments by contributing individual emission at the same wavelength. Hydrogel of Nmoc-F/FF and Nmoc-L/LL systems shows fluorescence decay lifetime 1.07 ns and 0.267 ns respectively (Table S1). The excitation wavelength was set at 367 nm and emission was monitored at 468 nm. The fluorescence decay lifetime of solution was found lowered as compared to hydrogels **1** and **2**, which indicates higher order aggregated nanofibrillar network [58] in the hydrogel (Figure S18). In the gel state, the peptides get aggregated to a more compact fashion. The peptides get assembled to a rigid framework into higher order structure through hydrogen bonding and π-stacking interactions, which results in increase in lifetime in hydrogel state.

We use oscillating rheometer to quantify the mechanical property of the hydrogels. The rheological measurement was performed with dynamic frequency sweep at a constant strain of

0.05% (Figure S19). Rheological measurements demonstrate the viscoelastic properties of hydrogel (Figure 10). The value of storage modulus G' exceeds over the loss modulus G'' by an order of magnitude, which confirms rigid and solid like behaviour of hydrogels.[59] The Nmoc-F/FF hydrogel system has higher G' value over the G'', which confirms rigid solid like hydrogel. However, the Nmoc-L/LL hydrogel system is slightly weaker than hydrogel **1**. Hydrogel **1** responses to gel-sol transition upon mechanical shaking and again restores its gel form upon resting. To quantify a thixotropic[60-61] property of hydrogel **1**, a simple step strain experiment was performed at constant angular frequency 10 rad s^{-1}. A constant strain 0.05% was applied for hydrogel **1**. Then the strain was slowly increased from 0.05 to 100%. The strain was kept constant for 2 min and 30 second, which resulted in gel-sol transition. The strain was decreased from 100% to 0.05% and the solution started to recover gelation property (G'> G'') within 1 min and 40 second. The storage modulus (G') was significantly found higher than the loss modulus (G''). The gel strength was recovered 65% of their original stiffness after removing strain (Figure 11). However, hydrogel **2** was unable to show thixotropic property.

Microscopic study is used to reveal the formation of nanostructures, which are responsible for hydrogel formation. The hydrogels were analysed by transmission electron microscope (TEM) and atomic force microscope (AFM). Hydrogel **1** shows nanofibrillar networks, which is confirmed by TEM (Figure 12A) and AFM (Figure 12B). A preferred gelator component in a DCL forms 3D nanofibrillar networks, which is capable to entrap large volumes of water. TEM analysis revealed that Nmoc-F/FF system self-assembled to form nanofibers[62] with diameter ranging from 35 to 45 nm (Figure 12A). AFM analysis revealed helical nanofibrillar morphology for hydrogel **1** with height ranging from 8 to 12 nm (Figure 12B). AFM analysis shows nanofibrillar morphology (Figure 13) for Nmoc-L/LL system. The average height for hydrogel **2**

nanofibers is 25 nm. The existence of interwoven morphology (Figure S20) indicates the formation of self-supporting hydrogel.

Conclusion

Here, we describe enzyme catalysed reverse hydrolysis reaction, which direct the peptide self-assembly in aqueous medium. Self-assembly brings up the amplification of a preferred library component over the non-assembling components. The peptides Nmoc-F_3 and Nmoc-L_5 evolved as major components for Nmoc-F/FF and Nmoc-L/LL systems. Nmoc-L/LLL system also depicts the formation of a preferred component Nmoc-L_5. The mechanical strength of the hydrogels was determined by rheological measurements, which indicate that both the hydrogels are strong and rigid. Hydrogen bonding as well as π-stacking interactions play major role in the self-assembly process. The Nmoc-F/FF and Nmoc-L/LL systems form fibrous networks, which is responsible for self-supporting hydrogel.

Experimental

Gel preparation

20 mmol of Nmoc-amino acid (Phe: F, Leu: L, Val: V and Ala: A) and 60 mmol of corresponding dipeptide and tripeptide (FF, LL, VV, AA and LLL) was suspended in 2 mL of 100 mmol sodium phosphate buffer (pH 8) in a glass vial. 1 mg mL^{-1} lyophilised thermolysin powder (bacillus Thermoproteolyticus rokko from Sigma-Aldrich) was added to the reaction mixture. The mixture was vortex mixed for 15 s to ensure dissolution. A self-supporting hydrogel was formed after 5 min for Nmoc-F/FF system whereas the hydrogel formed after 36 h for Nmoc-L/LL system.

HPLC Analysis

A Dionex HPLC-Ultimate 3000 (High Performance Liquid Chromatography) pump was used to analyse products. A 20 µL of sample was injected onto a Dionex Acclaim ® 120 C18 column of 250 mm length with an internal diameter of 4.6 mm and 5 µm fused silica particles at a flow rate of 1 mL min^{-1} (linear gradient of 40 % v/v acetonitrile in water for 35 min, gradually rising to 100 % (v/v) acetonitrile in water at 35 min). This concentration was kept constant until 40 min when the gradient was decreased to 40 % (v/v) acetonitrile in water at 42 min. The sample preparation involved mixing of 100 µL gel in 900 µL acetonitrile-water (50 : 50 mixture) solution containing 0.1 % trifluroacetic acid. The samples were then filtered through a 0.45 µm syringe filter (Whatman, 150 units, 13 mm diameter, 2.7 mm pore size) prior to injection. The products were identified by using Ultimate 3000 RS Variable Wavelength Detector at 280 nm.

UV-Vis spectroscopy

UV-Vis absorption spectra of the hydrogels **1** and **2** were recorded using a Varian Cary100 Bio UV-Vis spectrophotometer at a concentration of 20 mmol L^{-1}.

Fluorescence spectroscopy

Fluorescence emission spectra of gel (20 mmol L^{-1}) were recorded from 325-620 nm with excitation wavelength at 315 nm with medium sensitivity on a Horiba Scientific Fluoromax-4 spectrophotometer. The slit width for the excitation and emission was set at 2 nm and a 1 nm data pitch. Samples were prepared in 1 cm^2 quartz cuvette at room temperature.

Circular dichroism

Circular dichroism (CD) spectra were measured at 25 °C on a Jasco J-815 spectropolarimeter. Spectra were measured between 300 and 190 nm with a data pitch of 0.1 nm. The bandwidth was set to 1 nm with a scanning speed of 20 nm min^{-1} and a response time of 1 s. The path length was 1 mm quartz cell. Samples were prepared at a concentration of 2 mmol L^{-1}. Experimental data were acquired in thrice and the average data is shown. The CD data was obtained with the HT voltage less than 700 V.

FTIR

FTIR spectra were recorded using Bruker (Tensor 27) FT-IR spectrophotometer with spectral resolution of 4 cm^{-1}. All the measurements of gel samples were performed on crystal Zn-Se windows and scanned between 900 and 4000 cm^{-1} over 64 scans.

Rheology

Rheological study was performed to determine the mechanical properties of hydrogels. These properties were assessed using an Anton Paar Physica Rheometer (MCR 301, Austria) with cone plate geometry (20 mm in diameter, 50 μm gap and 1° angle) and temperature was controlled at 25 °C. The dynamic moduli of the hydrogel were measured as a function of frequency in the range of 0.1-100 rad s^{-1} with a constant strain value 0.05 %. To determine the exact strain for frequency sweep experiments, the linear viscoelastic (LVE) regime was performed at constant frequency of 10 rad s^{-1}. Experimental data was acquired in thrice and the average data is shown. 200 μL of gel was prepared in glass vial and transferred it over the plate using microspatula to

proceed for rheological measurements.

Morphological study

Transmission electron microscopic images were taken using a PHILIPS electron microscope (model: CM 200), operated at an accelerating voltage of 200 kV. Dilute solution of the gel was dried on carbon-coated copper grids (300 mesh) by slow evaporation in air and then allowed to dry separately in a vacuum at room temperature.

The morphology of gels was investigated using tapping mode atomic force microscope (AFM). AFM study was done by placing very dilute solution of gel (200 μL of gel was dissolved in 800 μL of milii-Q water) on mica and allowed it dry in air for 2 days at room temperature. Images were recorded by using scanning probe microscope AIST-NT instrument (model: Smart SPM-1000).

Time resolved study:

2 mL gel was prepared in a 1 cm^2 quartz cuvette and time resolved studies were done by a time correlated single photon counting (TCSPC) system from Horiba Yovin (Model: Fluorocube-01-NL). Samples were excited at 376 nm using a picosecond diode laser (Model: Pico Brite-375L). The signals were collected at magic angle (54.70) polarization using a photomultiplier tube (TBX-07C) as detector, which has a dark counts less than 20 cps. The instrument response function was typically 140 ps. The data analysis was performed using IBH DAS (version 6, HORIBA Scientific, Edison, NJ) decay analysis software.

The amplitude-weighted lifetime was estimated by

$$\langle \tau \rangle = \sum_{i=1}^{n} a_i \tau_i$$

where τ_1 is the fluorescence lifetime of various fluorescent species and are the a_1 normalized pre-exponential factors. To gain the best fitting in all cases the χ^2 was kept near to unity.

Acknowledgements

AKD thanks CSIR for funding this work. DBR and MK are indebted to CSIR and SB is indebted to UGC for their fellowship. We thank SAIF, IIT Bombay for the assistance of EM facility.

References

1. H. C. Fry, J. M. Grarcia, M. J. Medina, U. M. Ricoy, D. J. Gosztola, M. P. Nikiforov, L. C. Palmer and S. I. Stupp, *J. Am. Chem. Soc*. 2012, **134**, 14646-14649.
2. Y. Raz, B. Rubinov, M. Matmor, H. Rapaport, G. Ashkenasy and Y. Miller, *Chem. Commun*. 2013, **49**, 6561-6563.
3. D. M. Ryan and B. L. Nilsson, *Polym. Chem.* 2012, **3**, 18-33.
4. J. Y. Lee, Y. M. Kang, E. Kim, M. L. Kang, B. Lee, J. H. Kim, B. H. Min, K. Park and M. S. Kim, *J. Mater. Chem*. 2010, **20**, 3265-3271.
5. Z. Yang, G. Liang, M. Ma, A. S. Abbah, W. W. Lu and B. Xu, *Chem. Commun*. 2007, 843-845.
6. D. Ma, K. Tu and L. M. Zhang, *Biomacromolecules* 2010, **11**, 2204-2212.
7. J. R. Li, J. Sculley and H. C. Zhou, *Chem. Rev.* 2012, **112**, 869-932.
8. H. Hosseinkhani, P.-D. Hong and D.-S. Yu, *Chem. Rev.* 2013, **113**, 4837-4861.
9. C. A. E. Hauser and S. Zhang, *Chem. Soc. Rev.* 2010, **39**, 2780-2790.
10. L. Haines-Butterick, K. Rajagopal, M. Branco, D. Salick, R. Rughani, M. Pilarz, M. S. Lamm, D. J. Pochan and J. P. Schneider, *Proc. Natl. Acad. Sci. U. S. A.*, 2007, **104**, 7791-7796.
11. L. A. Estroff and A. D. Hamilton, *Chem. Rev*. 2004, **104**, 1201-1217.
12. N. M. Sangeetha and U. Maitra, *Chem. Soc. Rev*. 2005, **34**, 821-836.
13. S. Kiyonaka, K. Sugiyasu, S. Shinkai and I. Hamachi, *J. Am. Chem. Soc*. 2002, **124**, 10954-10955.

14. M. D. Segarra-Maset, V. J. Nebot, J. F. Miravet and B. Escuder, *Chem. Soc. Rev.* 2013, **42**, 7086-7098.
15. I. Maity, D. B. Rasale and A. K. Das, *Soft Matter*, 2012, **8**, 5301-5308.
16. F. Versluis, H. R. Marsden and A. Kros, *Chem. Soc. Rev.* 2010, **39**, 3434-3444.
17. Z. Yang, G. Liang, L. Wang and B. Xu, *J. Am. Chem. Soc*. 2006, **128***,* 3038-3043.
18. J. Gao, H. M. Wang, L. Wang, J. Y. Wang, D. L. Kong and Z. M. Yang, *J. Am. Chem. Soc*. 2009, **131**, 11286-11287.
19. J. H. Collier and P. B. Messersmith, *Bioconjugate Chem.* 2003, **14**, 748-755.
20. P. T. Corbett, J. Leclaire, L. Vial, K. R. West, J. Wietor, J. K. M. Sanders and S. Otto, *Chem. Rev*. 2006, **106***,* 3652-3711.
21. S. Ladame, *Org. Biomol. Chem*. 2008, **6**, 219-226.
22. J. M. Lehn, *Chem. Soc. Rev*. 2007, **36***,* 151-160.
23. P.Vongvilai, M. Angelin, R. Larsson and O. Ramstrom, *Angew. Chem., Int. Ed*. 2007, **46**, 948-950.
24. S. M. Turega, C. Lorenz, J. W. Sadownik and D. Philp, *Chem. Commun*. 2008, 4076-4078.
25. N. A. Stephenson, J. Zhu, S. H. Gellman and S. S. Stahl, *J. Am. Chem. Soc.* 2009, **131**, 10003-10008.
26. H. J. Cooper, M. A. Case, G. L. McLendon and A. G. Marshall, *J. Am. Chem. Soc.* 2003, **125**, 5331-5339.
27. R. T. S. Lam, A. Belenguer, S. L. Roberts, C. Naumann, T. Jarrosson, S. Otto and J. K. M. Sanders, *Science* 2005, **308**, 667-669.
28. P. J. Boul, P. Reutenauer and J. M. Lehn, *Org. Lett.* 2005, **7**, 15-18
29. R. J. Lins, S. L. Flitsch, N. J. Turner, E. Irving and S. A. Brown, *Angew. Chem. Int. Ed.* 2002, **41**, 3405-3407.
30. J. Hu, G. Zhang and S. Liu, *Chem. Soc. Rev.* 2012, **41**, 5933-5949.
31. S. Toledano, R. J. Williams, V. Jayawarna and R. V. Ulijn, *J. Am. Chem. Soc.* 2006, **128**, 1070-1071.
32. R. J. Williams, A. M. Smith, R. Collins, N. Hodson, A. K. Das and R. V. Ulijn, *Nature Nanotech.* 2009, **4**, 19-24.
33. S. K. M. Nalluri and R. V. Ulijn, *Chem. Sci.* 2013, **4**, 3699-3705.
34. L. Chronopoulou, S. Lorenzoni, G. Masci, M. Dentini, A. R. Togna, G. Togna, F. Bordic and C. Palocci, *Soft Matter* 2010, **6**, 2525-2532.
35. L. Chronopoulou, A. R. Togna, G. Guarguaglini, G. Masci, F. Giammaruco, G. I. Togna and C. Palocci, *Soft Matter* 2012, **8**, 5784-5790.
36. M. G. Simpson, M. Pittelkow, S. P. Watson and J. K. M. Sanders, *Org. Biomol. Chem.* 2010, **8,** 1181-1187.
37. J. M. A. Carnall, C. A. Waudby, A. M. Belenguer, M. C. A. Stuart, J. J.-P. Peyralans and S. Otto, *Science* 2010, **327,** 1502-1506.
38. N. Sreenivasachary and J. M. Lehn, *Proc. Natl. Acad. Sci. U.S.A*. 2005, **102**, 5938-5943.

39. R. Orbach, L. Adler-Abramovich, S. Zigerson, I. Mironi-Harpaz, D. Seliktar and E. Gazit, *Biomacromolecules* 2009, **10**, 2646-2651.
40. Y. Zhang, H. Gu, Z. Yang and B. Xu, *J. Am. Chem. Soc.* 2003, **125**, 13680-13681.
41. D. B. Rasale, I. Maity and A. K. Das, *RSC Adv.* 2012, **2**, 9791-9794.
42. H. Wang, C. Yang, M. Tan, L. Wang, D. Kong and Z. Yang, *Soft Matter* 2011, **7,** 3897-3905.
43. L. Chen, S. Revel, K. Morrisb and D. J. Adams, *Chem. Commun*. 2010, **46**, 4267-4269.
44. K. Elfrink, J. Ollesch, J. Sçhr, D. Willbold, D. Riesner and K. Gerwert, *Proc. Natl. Acad. Sci. U. S. A.* 2008, **105**, 10815-10819.
45. M. S. Lamm, K. Rajagopal, J. P. Schneider and D. J. Pochan, J. *Am. Chem. Soc.* 2005, **127**, 16692-16700.
46. X. Yan, Y. Cui, Q. He, K. Wang, and J. Li, *Chem. Mater.* 2008, 20*,* 1522-1526.
47. B. Kim, S. Choi, S. Han, K. Choi and Y. Lim, *Chem. Commun.* 2013, 49, 7617-7619.
48. S. G. Tarasova, V. Gaponenkob, O. M. Z. Howard, Y. Chenc, J. J. Oppenheimc, M. A. Dybaa, S. Subramaniame, Y. Leeb, C. Michejdaa and N. I. Tarasova, *Proc. Natl. Acad. Sci. U. S. A* 2011, **108**, 24, 9798-9803.
49. E. F. Banwell, E. S. Abelardo, D. J. Adams, M. A. Birchall, A. Corrigan, A. M. Donald, M. Kirkland, L. C. Serpell, M. F. Butler and D. N. Woolfson, *Nature Mater.* 2009, **8**, 596-600.
50. P. Moitra, K. Kumar, P. Kondaiah and S. Bhattacharya, *Angew. Chem. Int. Ed.* 2013, **52**, 1–6
51. X. Yan, Y. Cui, Q. He, K. Wang and J. Li, *Chem. Mater.,* 2008, **20**, 1522-1526.
52. C.-S. Chen, T.-J. Ji, X.-D. Xu, X.-Z. Zhang and R.-X. Zhuo, *Macromol. Rapid Commun*. 2010, **31**, 1903-1908.
53. Y. Lim, K. Moon and M. Lee, *Angew. Chem. Int. Ed.* 2009, **48**, 1601-1605.
54. H. Cao, X. Zhu and M. Liu, *Angew. Chem. Int. Ed.* 2013, **52,** 4122-4126.
55. Y. Kuang, Y. Gao, J. Shi, H. Lin and Bing Xu, *Chem.Commun*. 2011, **47**, 8772-8774.
56. Z. Yang, L. Wang, J. Wang, P. Gao and Bing Xu, *J. Mater. Chem*. 2010, **20**, 2128-2132.
57. A. K. Das, A. R. Hirst and R. V. Ulijn, *Faraday Discuss.* 2009, **143**, 293-303.
58. I. Maity, T. K. Mukherjee and A. K. Das, *New J. Chem.* 2014, **38**, 376-385.
59. S. Roy and A. Banerjee, *Soft Matter* 2011, **7**, 5300-5308.
60. S. Basak, J. Nanda, and A. Banerjee, *Chem. Commun*. 2014, **50**, 2356-2359.
61. Y. Ohsedo, M. Oono, K. Saruhashib and H. Watanabeab, *RSC Adv*. 2014, **4**, 48554-48558.
62. J. Li, Y. Gao, Y. Kuang, J. Shi, X. Du, J. Zhou, H. Wang, Z. Yang and B. Xu, *J. Am. Chem. Soc*. 2013, **135**, 9907-9914.

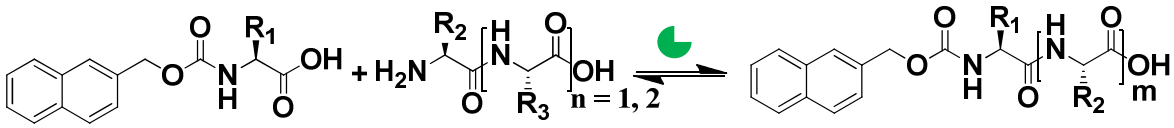

Scheme 1. Enzyme catalyzed reverse hydrolysis reaction of Nmoc-Amino acids with di, tripeptides, which evolve dynamic peptide libraries.

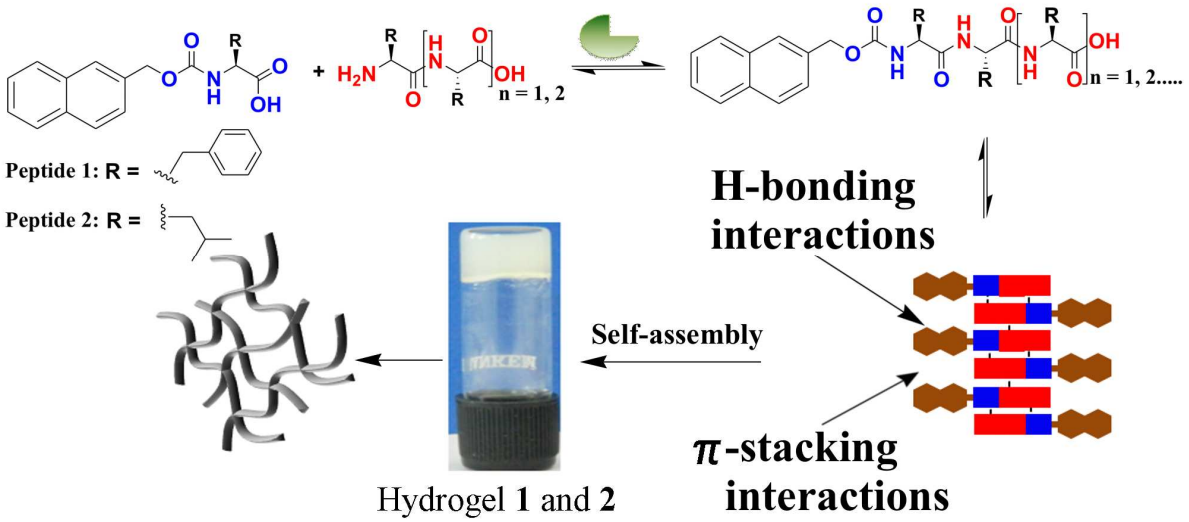

Figure 1. Enzyme catalyzed reverse hydrolysis reaction of Nmoc-amino acids and dipeptides. The schematic representation describes enzyme-catalysed evolution of dynamic peptide libraries of Nmoc-F/FF and Nmoc-L/LL systems. Enzyme catalysed amplification of Nmoc-F_3 of Nmoc-F/FF system and Nmoc-L_5 of Nmoc-L/LL system self-assemble to form nanostructures in gel phase.

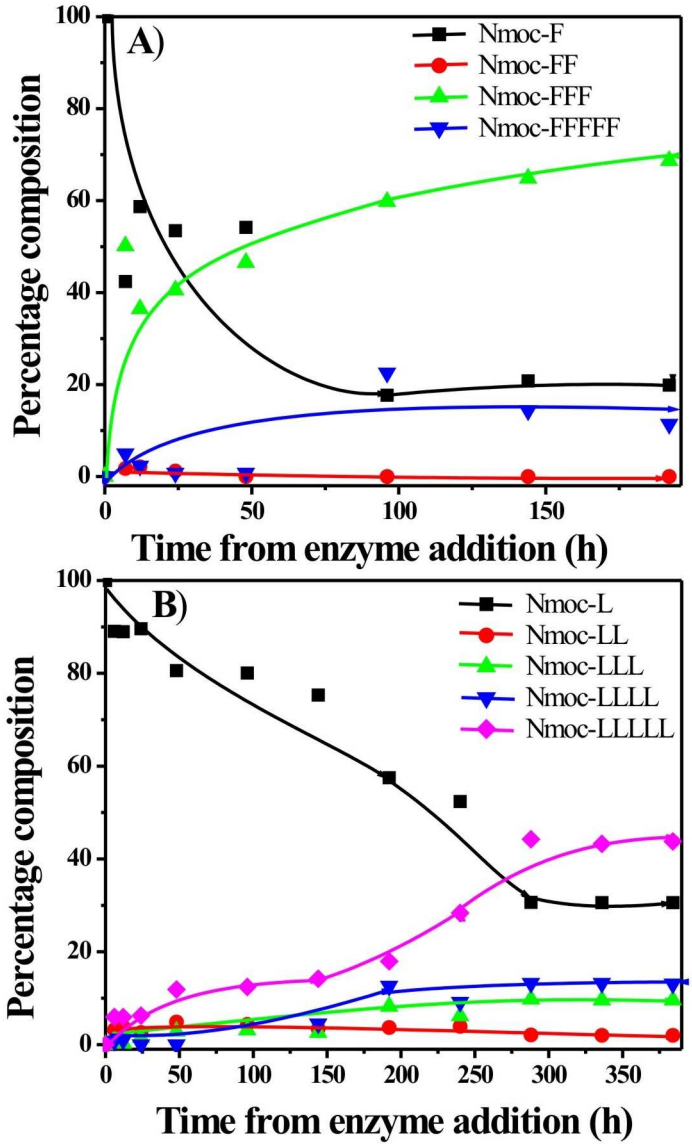

Figure 2. Time course of the conversion of peptide oligomers in dynamic combinatorial libraries of A) Nmoc-F/FF system and B) Nmoc-L/LL system.

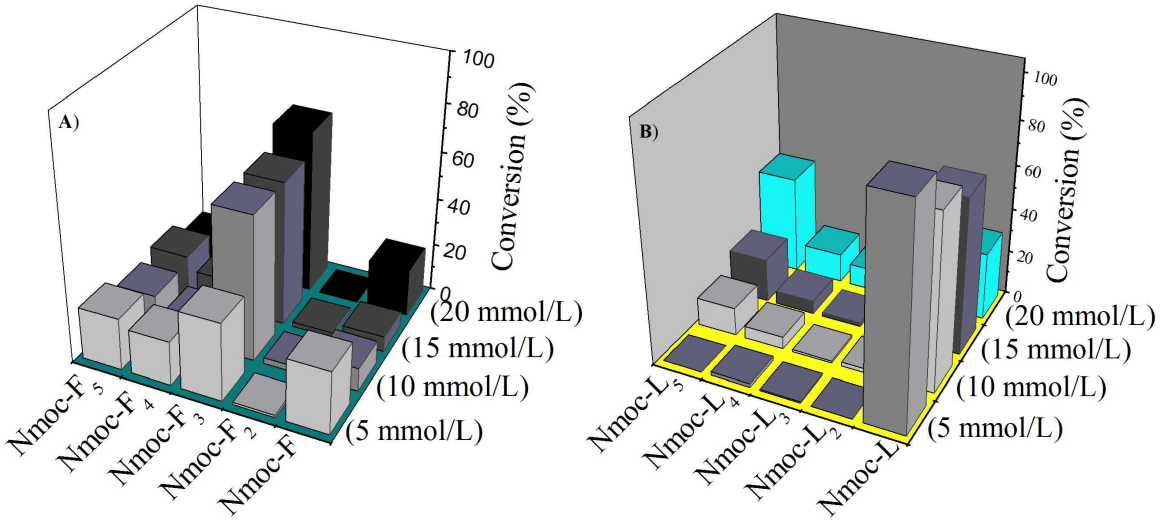

Figure 3. The formation of peptide oligomers from enzyme catalyzed dynamic library of (A) Nmoc-F/FF and (B) Nmoc-L/LL systems at different concentrations.

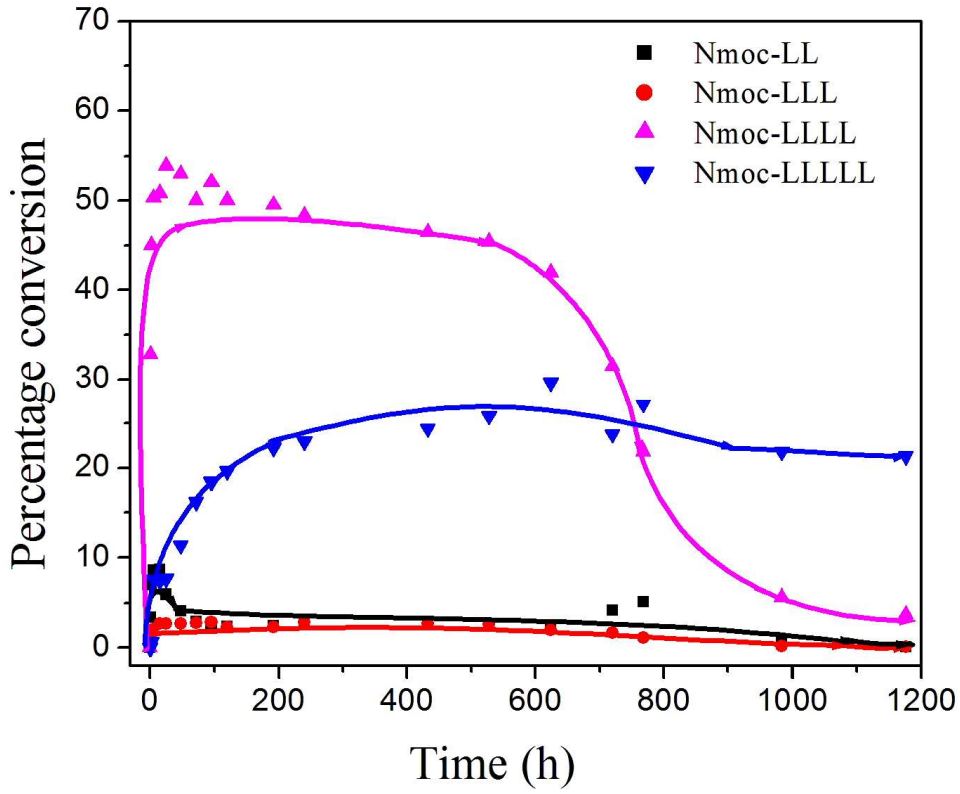

Figure 4. Real time conversion of peptide oligomers in a dynamic peptide library of Nmoc-L/LLL system.

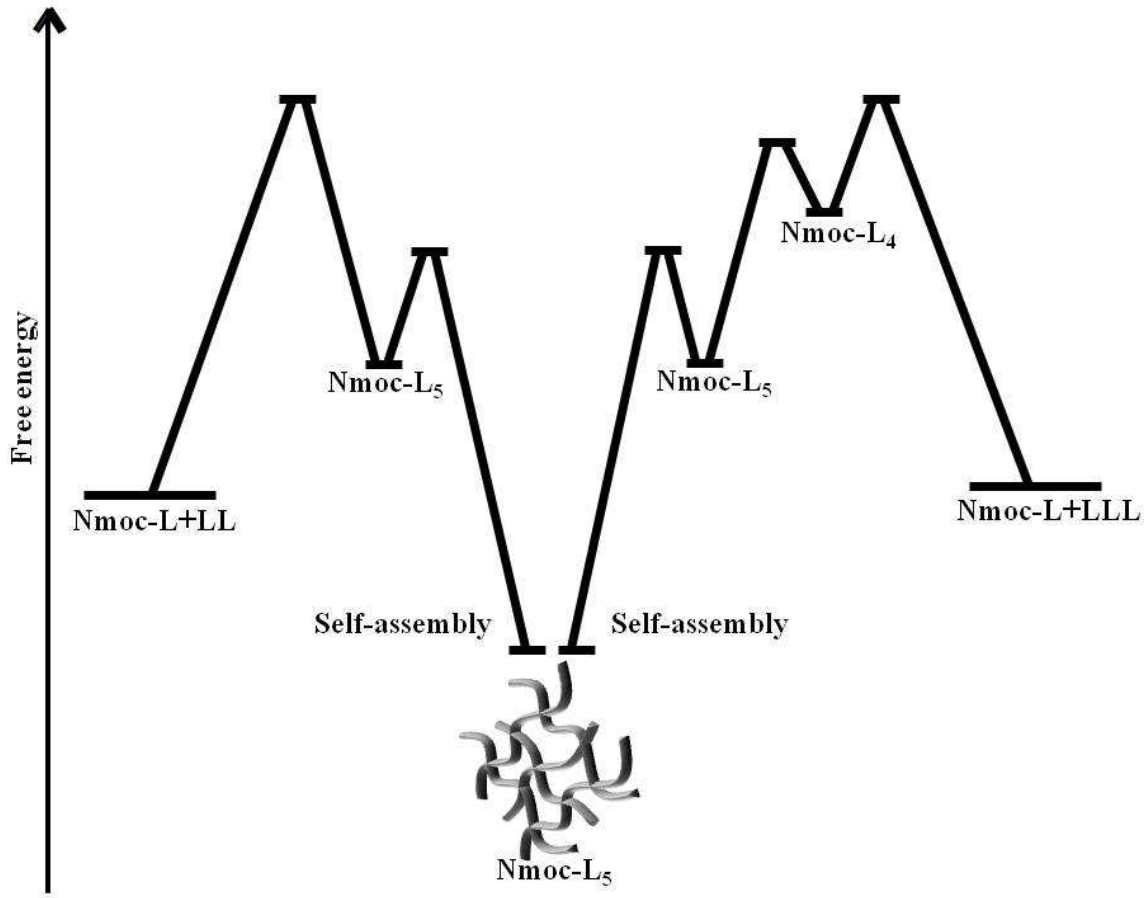

Figure 5. Free energy profile diagram of enzyme catalysed dynamic peptide libraries. Nmoc-L/LL system leads to form Nmoc-L_5 via amide bond formation which subsequently self-assembles to form nanofibrillar structures. Nmoc-L/LLL initially forms Nmoc-L_4 which leads to form thermodynamically favoured Nmoc-L_5 followed by self-assembly.

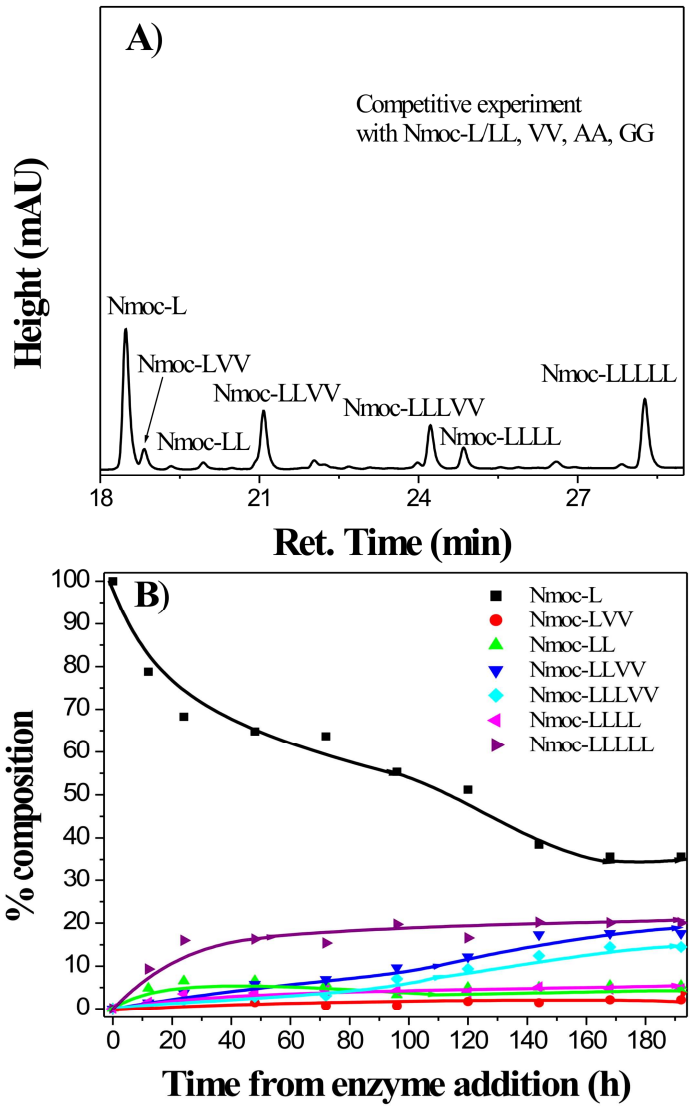

Figure 6. A) High performance liquid chromatography (HPLC) analysis for Nmoc-L/LL, VV, AA and GG system, which form dynamic library of peptides upon treatment with thermolysin after 8 days. B) Time course of the conversion of peptide oligomers in dynamic combinatorial libraries of Nmoc-L/LL, VV, AA and GG system.

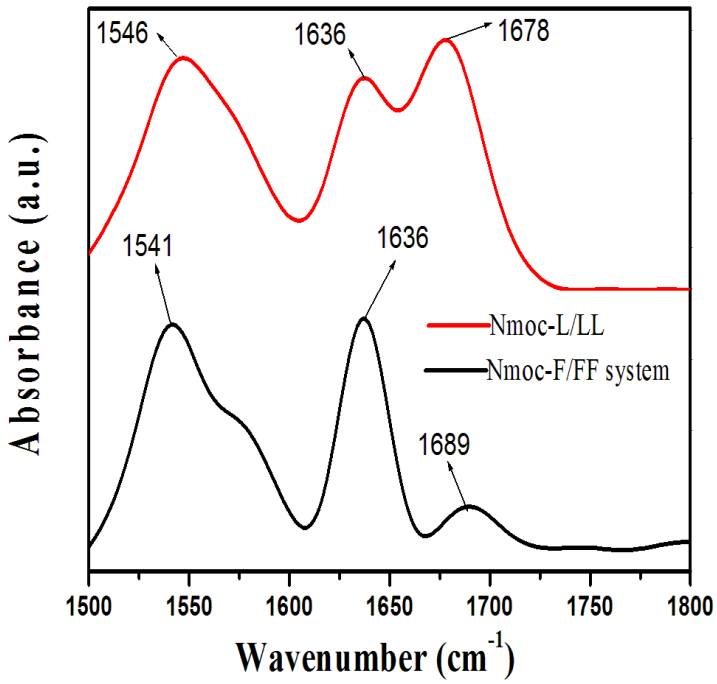

Figure 7. FTIR spectra of self-assembled peptides Nmoc-F_3 and Nmoc-L_5 obtained from systems Nmoc-F/FF at 8 days and Nmoc-L/LL at 16 days. The peaks in amide I region indicate β-sheet conformation in gel phase.

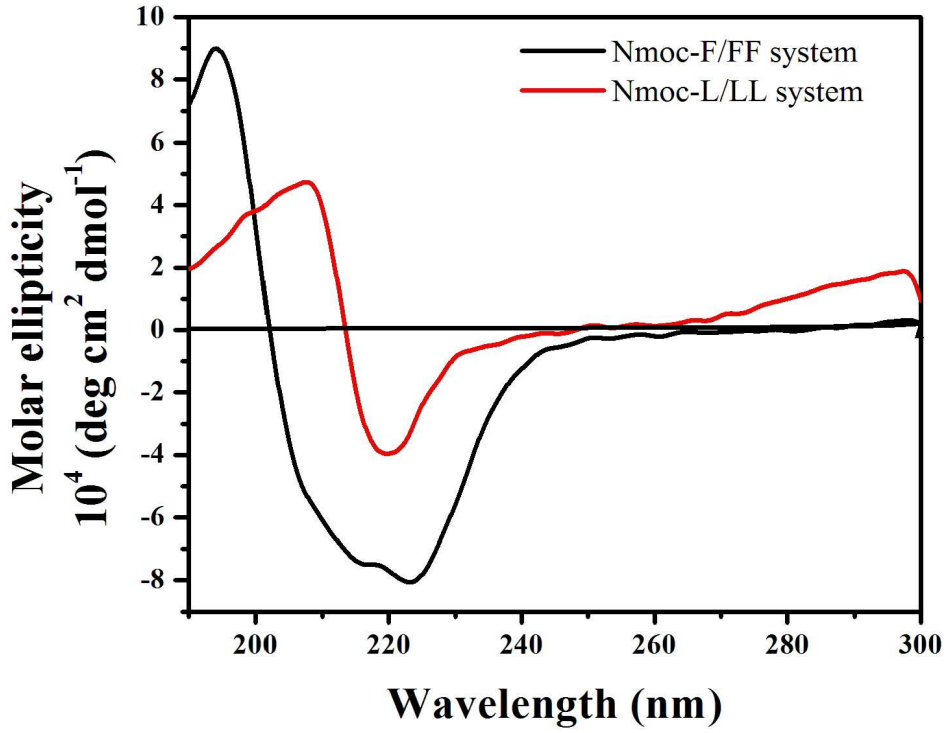

Figure 8. A) Circular dichorism (CD) spectra of hydrogels **1** at 8 days and **2** at 16 days reveal the formation of β-sheet and helical structures through extensive hydrogen-bonding interactions.

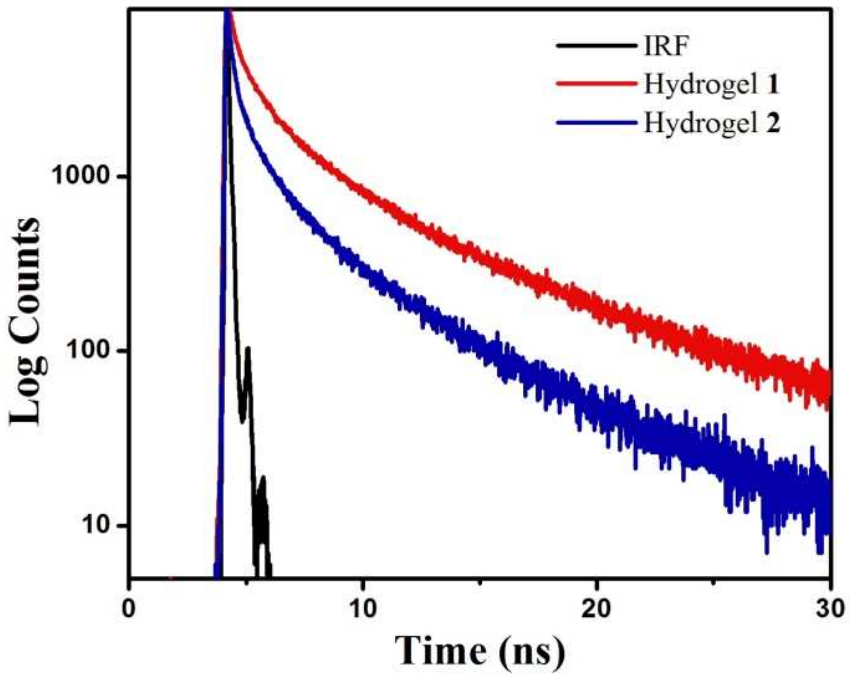

Figure 9. Emission decay curves of hydrogels **1** and **2** (concentration 20 mmol L^{-1}) monitored at 468 nm (λ_{ex} = 367 nm). The decay curve was recorded after 24 h of enzyme reaction. (IRF: instrument response function)

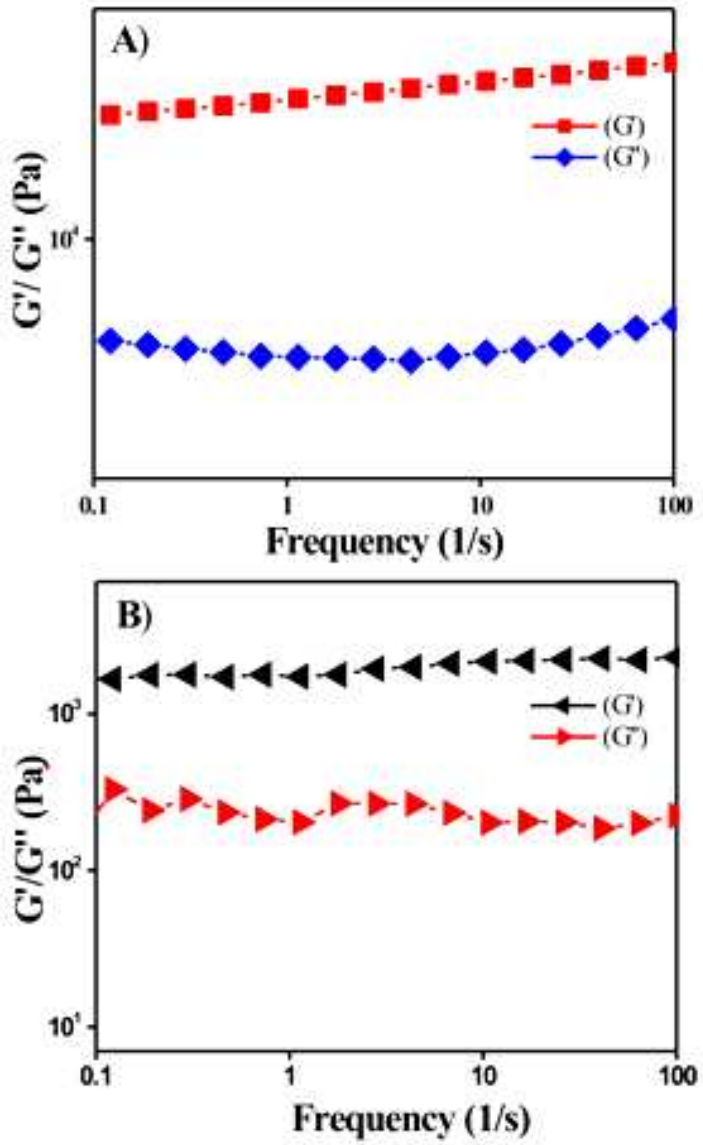

Figure 10. Dynamic frequency sweep of A) hydrogel **1** and B) hydrogel **2** indicates that storage modulus (G') is higher than the loss modulus (G'') which confirms the rigidity of hydrogel at a constant strain of 0.05%.

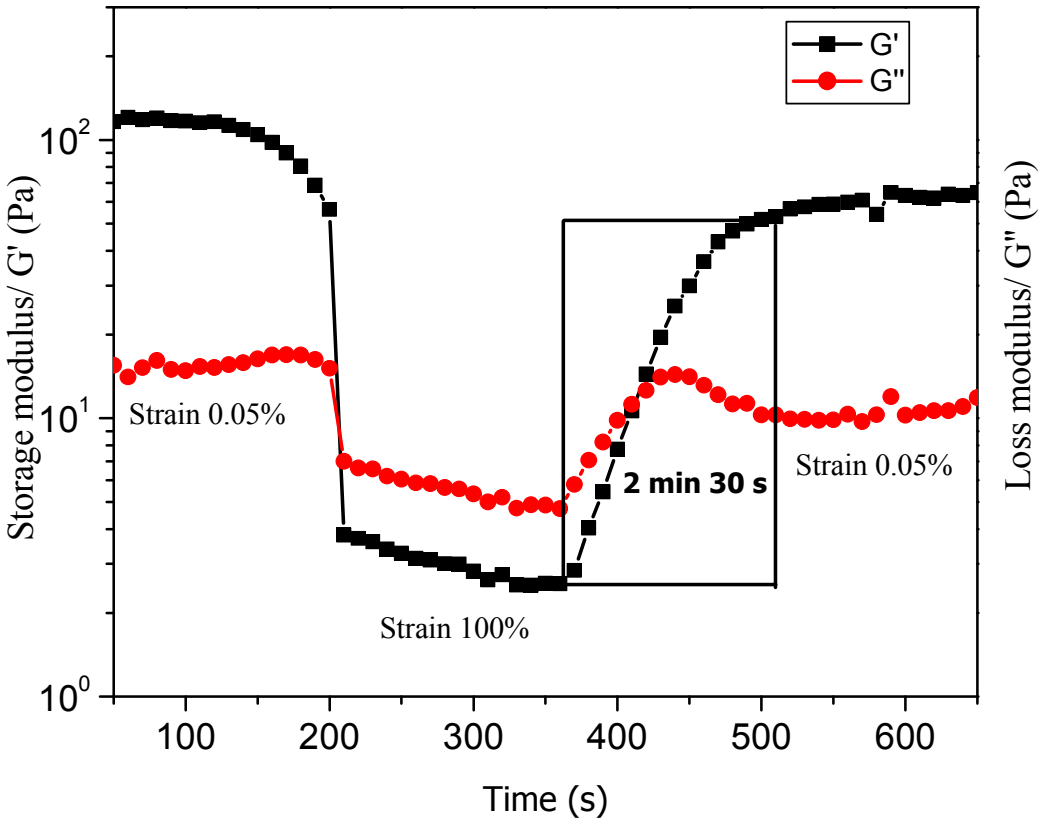

Figure 11: Step strain experiment demonstrates the thixotropic property of hydrogel **1.** Variation of storage modulus and loss modulus was observed under the application and withdrawal of strain in stepwise manner.

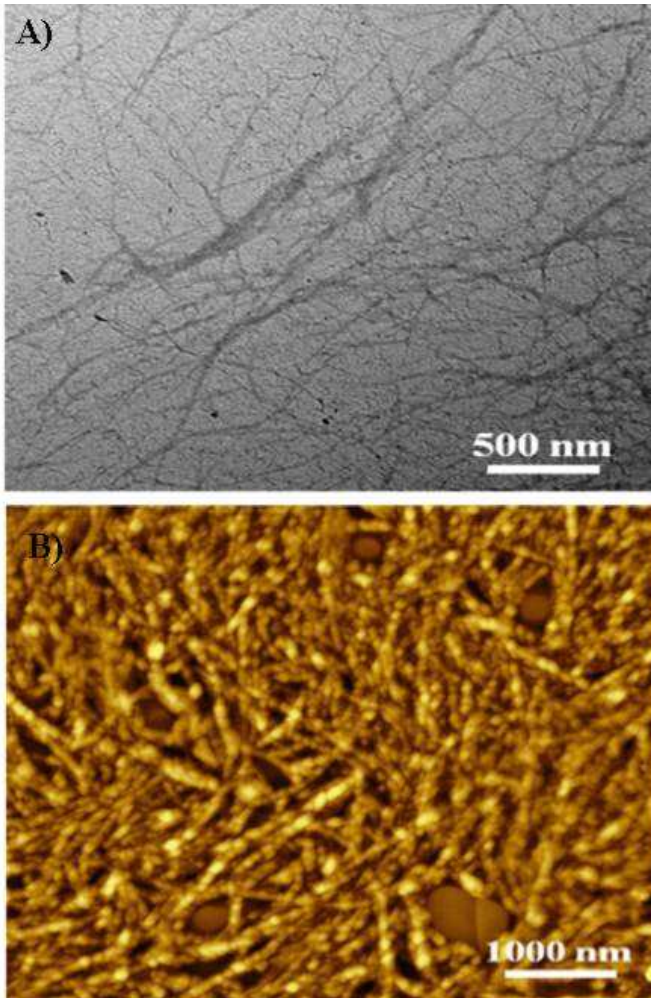

Figure 12. A) TEM image of hydrogel **1** shows nanofibrillar morphology. B) AFM image of hydrogel **1** indicates helical nanofibers.

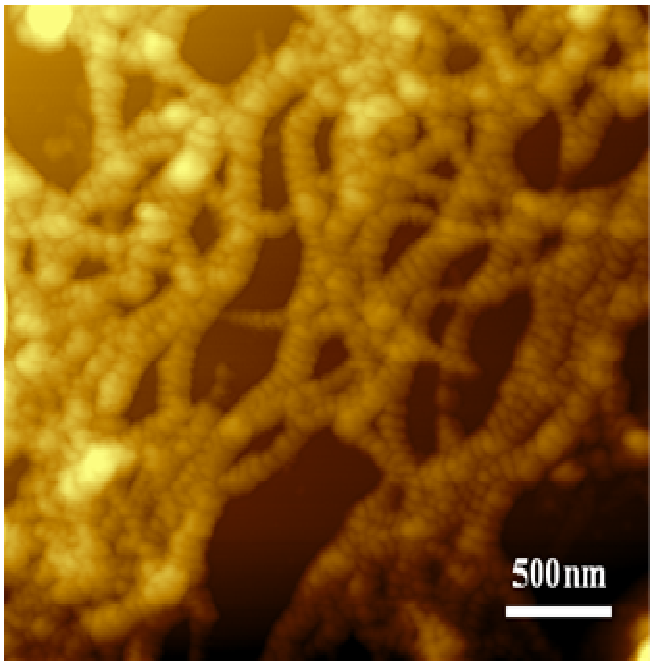

Figure 13. AFM image of hydrogel **2** shows nanofibrillar morphology.

Table1: Product formation upon biocatalytic reverses hydrolysis reaction

Entry	Starting	Enzyme	Nmoc-X %	Nmoc-X_2 %	Nmoc-X_3 %	Nmoc-X_4 %	Nmoc-X_5 %
1.	Nmoc-F + FF	1 mg/mL	18.56	0	71.29	3.77	6.39
2.	Nmoc-L + LL	1 mg/mL	30.82	2.02	9.58	13.30	44.28
3.	Nmoc-V + VV	1 mg/mL	100	0	0	0	0
4.	Nmoc-A + AA	1 mg/mL	100	0	0	0	0
5.	Nmoc-L + LLL	1 mg/mL	74.81	0.12	0.1	3.68	21.29

Nmoc: Naphthalene-2-methoxycarbonyl, X = Phenylalanine (entry 1); X = Leucine (entry 2 and 5); X = Valine (entry 3) and X = Alanine (entry 4)

Table of Contents

Exploring Thermodynamically Downhill Nanostructured Peptide Libraries: From Structural to Morphological Insight

*Dnyaneshwar B. Rasale, Sagar Biswas, Maruthi Konda and Apurba K. Das**

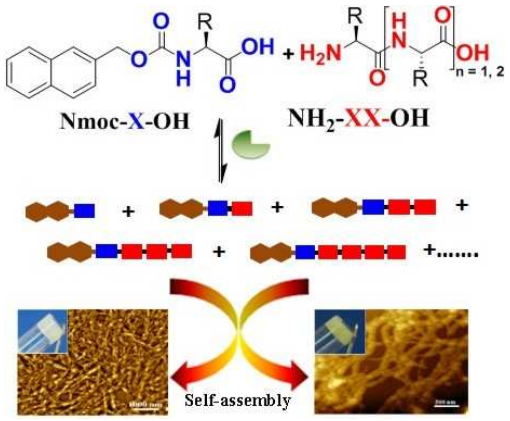

Biocatalytic evolution of Nmoc (naphthalene-2-methoxycarbonyl)-capped dynamic combinatorial libraries in peptide hydrogels were envisaged. The reversible enzymatic reactions lead to generate preferred nanostructured components through peptide self-assembly.